

Supporting Information

Integrin Subtypes and Nanoscale Ligand Presentation Influence Drug Sensitivity in Cancer Cells

Jennifer L. Young^{†,‡}, Ximeng Hua^{†,‡}, Heidi Somsel^{†,‡}, Florian Reichart[§], Horst Kessler[§], and Joachim P. Spatz^{†,‡,}*

[†]Department of Cellular Biophysics, Max Planck Institute for Medical Research, 69120 Heidelberg, Germany

[‡]Department of Biophysical Chemistry, Heidelberg University, 69120 Heidelberg, Germany

[§]Department of Chemistry, Technical University of Munich, 85748 Garching, Germany

*spatz@mr.mpg.de; +49 6221 486-420

Contents

	Page #
1. Materials and Methods.....	S3-S5
2. Supporting Experiments.....	S5
3. Supplemental Figures.....	S6-S12
4. Tables of Significance Comparisons.....	S13-S15
5. Supporting References.....	S15

Materials and Methods

Protein functionalized surfaces. White-walled tissue culture treated plastic 96-well plates (Greiner Bio-One) were coated with 10 $\mu\text{g}/\text{mL}$ human plasma fibronectin (Roche) or human plasma vitronectin (Promega) in sterile 1X PBS overnight at 4°C with gentle shaking to ensure a uniform layer was deposited. After incubation, plates were rinsed two times with sterile 1X PBS. 1% BSA (Serva) dissolved in sterile 1X PBS was added for 15 min at 37°C in order to prevent non-specific cell binding to any potentially remaining exposed surface. Plates were rinsed again three times with sterile 1X PBS then sterilized under UV for 30 min before cell plating.

Preparation of AuNP arrays. Block copolymer micelle nanolithography (BCMn) was utilized to produce hexagonally ordered gold nanoparticle (AuNP) arrays as described previously¹. Briefly, CARO solution (3:1 sulphuric acid:hydrogen peroxide) was used to clean borosilicate glass slides of 25 x 85 x 1 mm (cut in-house, for survival and motility assays) or 12 mm \varnothing #1 borosilicate glass coverslips (Roth, for immunofluorescence experiments) for 2 hr, followed by extensive rinsing and sonication in MiliQ H₂O. Gold micellar solutions were produced by dissolving polystyrene-b-poly(2-vinylpyridine) (P2VP) diblock copolymer (Polymer Source) in o-xylene and subsequently loading micelles with HAuCl₄·3H₂O (Sigma Aldrich) at $L = 0.3 - 0.5$ according to $L = n [\text{HAuCl}_4] / n [\text{P2VP}]$. The glass substrates were then spin-coated with 12 μL (for 12 mm \varnothing coverslips) or 120 μL (for 25 x 85 mm slides) of the gold micellar solution using a WS-650HZ-23NPP/A2/AR2 spin coater (Laurell Technologies Cooperation, USA). The samples were then treated with argon/hydrogen plasma (90% Ar/10% H₂) in a Tepla PS210 microwave plasma system (PVA Tepla, Germany) for 45 min at 350 W and 0.4 mbar in order to remove the copolymer. The theoretical repeat units of PS (288 or 501), the concentration of copolymer (3 - 5 mg/mL), and the spin speed (3,000 – 8,000 rpm) were all optimized to produce surfaces with uniform AuNP spacing of 35, 50 and 70 nm. Theoretical repeat units of P2VP were kept constant at 119.

Peptide functionalization of AuNP array-coated substrates. In order to avoid potential protein adsorption and cell attachment onto the glass surface between the AuNPs, surfaces were activated with O₂ plasma for 10 min at 150 W and 0.4 mbar and directly passivated by adding 0.25 mg/mL PLL(20)-g[3.5]-PEG(2) (SuSoS Surface Technology, Switzerland) dissolved in HEPES buffer (10 mM, pH 7.4) for 45 min, then rinsed in MiliQ H₂O and dried under N₂ flow. Under sterile conditions, 16-well ProPlate[®] molds (Grace Bio-labs, USA) were mounted onto the AuNP glass slides, while coverslips were placed in a petri dish, then all samples were rinsed 3X with sterile MiliQ H₂O. 50 μL of 25 μM peptidomimetics dissolved in sterile MiliQ H₂O were added to each well/coverslip for 2 hr at RT. The wells were then rinsed 2X with water, then 2X with sterile 1X PBS before cell plating. Controls either without AuNPs or bare AuNPs were also included in each experiment in order to confirm successful passivation (in the former case) or peptidomimetic-specific binding of cells (in the latter case).

Characterization of AuNP substrates. After plasma treatment, samples were characterized via scanning electron microscopy (SEM) for spacing vs. spin speed and organization of nanoparticles. SEM samples were sputter-coated with ~ 7 nm of carbon (Low Vacuum Coater EM ACE200, Leica) and imaged in an Ultra 55FE-SEM mounted with a Gemini column (Carl Zeiss) using an in-lens detector at an accelerating voltage of 5 kV and working distance of ~ 6 mm. For each sample, at least three images distributed across the surface were taken and were subsequently

quantified for both interparticle spacing and hexagonal order ($k = 6$) via calculation of the k -nearest neighbors as described previously. A custom script in Fiji was utilized, with each image containing $\sim 600 - 2,500$ particles, depending on spacing. Samples with AuNP spacing of 35, 50 and 70 nm with uniform, hexagonal arrangement determined by the 6-fold bond orientational order parameter, as previously described², were utilized.

Cell culture. MDA-MB-231s (ATCC) were maintained in DMEM (Gibco) supplemented with 10 % fetal bovine serum (FBS, Sigma), 1 % non-essential amino acids (Gibco) and 1 % Penicillin-Streptomycin (Gibco) in a sterile, humidified incubator at 37°C and 5 % CO₂. For initial integrin blocking and cell plating, media with only 1% FBS was used in order to avoid non-specific interactions. After trypsinization (0.05% Trypsin-EDTA, Gibco; 4 min at 37°C), cells were counted using a Z2 Coulter Particle Count and Size Analyzer (Beckman Coulter, USA), and then plated at a density of 150 cells/mm². For blocking experiments, cells were re-suspended in 1/5 of the final plating volume required and peptidomimetics were added at 50 μ M for 10 min on ice. Warm media was then added up to the final volume such that the peptidomimetics were at 10 μ M and the cells were plated. Cells were allowed to adhere for 3 hr, at which point media was exchanged for 10 % FBS media with or without drugs. 5-Fluorouracil (5-FU; Sigma-Aldrich) was added at 100 μ M and Paclitaxel (Acros Organics) was added at 50 nM to elicit ~ 50 % cell death (Fig. S5). Negative controls were prepared according to the solution in which the drugs were dissolved, i.e. PBS for 5-FU and DMSO for Paclitaxel. If peptidomimetics were used, they were also added into the media exchange at a concentration of 10 μ M.

Immunofluorescence microscopy. In order to examine cell morphology, focal adhesion (FA) area, and confirm integrin-specific binding, immunofluorescence was performed. Cells were fixed in 3.7 % paraformaldehyde in PBS for 20 min, rinsed 3X in PBS, and permeabilized with 1 % Triton-X 100 in PBS for 10 min. Cells were rinsed in 1 % PBS-T (1X PBS with 1 % Tween) 3X and then stained with the following primary antibodies depending on the experiment at a dilution of 1:250 in 1 % BSA in PBS-T at 4°C overnight: Anti-paxillin [Y113] rabbit monoclonal antibody (Abcam ab32084, UK); Anti-integrin alpha V beta 3 mouse monoclonal antibody [LM609] (Abcam ab190147, UK); Anti-integrin alpha 5 rabbit monoclonal antibody [EPR7854] (Abcam ab150361, UK). Following 3X rinse in PBS-T, samples were incubated with the following secondary antibodies: Chicken anti-rabbit Alexa Fluor[®] 488 (Life Technologies), Goat anti-mouse Alexa Fluor[®] 647 (Life Technologies), and Alexa Fluor[®] 568 phalloidin (for actin, Invitrogen) at 1:1000 at RT for 2 hr. Samples were then rinsed 3X in MiliQ H₂O and mounted in Fluoromount-G[®] w/DAPI (Southern Biotech) and sealed with a #1 coverslip. Imaging was performed on a Zeiss Axiovert 200M (Carl Zeiss AG, Germany) using an oil-immersion 63X objective for FA visualization and a 10X objective for cell morphology visualization, captured with AxioVision Rel. 4.8 software.

Live cell microscopy. After plating cells on functionalized substrates, plates were moved to an Axio Observer.Z1 (Carl Zeiss AG, Germany) microscope fitted with a custom-built cell incubation chamber so that imaging could proceed in a humidified, 37°C, and 5 % CO₂ environment. Phase contrast images were taken at 3 - 4 points per sample every 10 minutes for 72 hr using AxioVision Rel. 4.8 software. Movies of cells migrating were analyzed in Imaris (Bitplane) software.

Survival and proliferation assay. Cells treated with chemotherapeutic drugs were examined for survival using the CellTiter-Glo[®] Luminescent Cell Viability Assay (Promega) in which the measured luminescent signal is proportional to the amount of ATP present, which is directly proportional to the number of cells in culture. After drug treatment, cell culture plates were stabilized to room temperature for 30 min, the CellTiter-Glo[®] Reagent was added at a 1:1 ratio to media (i.e. 100 μ L media + 100 μ L reagent), the plate was mixed to induce cell lysis for 2 min, the luminescent signal was stabilized for 10 minutes at room temperature, and luminescence was recorded with an integration time of 1 second per well. Control wells (media alone, with and without drugs, plus reagent) were also prepared to account for any experiment-specific background. The concentration of drugs used, i.e. 5-Fluorouracil at 100 μ M and Paclitaxel at 50 nM, was shown to elicit ~ 50 % cell death from a drug dose experiment (Fig. S5). Proliferation based on integrin subtype engagement on fibronectin (via performing blocking experiments) at 3 and 48 hr was also assessed (Fig. S4).

Image and statistical analyses. Immunofluorescent 63X images were analyzed in Fiji³ for FA morphology and 10X images were analyzed in CellProfiler⁴ for cell morphology. Cell numbers analyzed indicated in corresponding figure captions. For live cell experiments, after acquiring time lapse videos, cells were tracked and analyzed using Imaris (Bitplane) software for xy speed (μ m/min). Roseplots representing 17 hrs of culture (in order to better visualize tracks) were created using the XTension Pack for Advanced Object Movement Analysis. All statistical analyses were performed using one-way or two-way ANOVA or student's t-test, as indicated, using Prism (GraphPad) Software. Statistical differences among groups were assessed to identify the interaction between spacing, drug treatment, and integrin subtype-specific peptidomimetics when $p < 0.05$. All data is presented as mean \pm 95% confidence interval (CI) or standard error of the mean (sem) as indicated from triplicate biological experiments with at least 2 technical replicates per sample, unless otherwise indicated. All significance comparisons from Figures 1 C-F and 2 C-F are displayed in Tables S1 and S2, respectively.

Supporting Experiments

Peptidomimetic specificity. While the integrin-specificity of our synthesized peptidomimetics has been confirmed previously⁵, we ensured functionality in our system by performing immunofluorescence staining of integrins $\alpha_v\beta_3$ or $\alpha_5\beta_1$ to observe integrin expression patterns, i.e. when engaging $\alpha_5\beta_1$, the presence of $\alpha_v\beta_3$ was greatly reduced and vice versa (Fig. S2A). As an additional control, cells were plated on vitronectin (Vn), in which $\alpha_v\beta_3$ is the major binding integrin, and treated with the $\alpha_v\beta_3$ peptidomimetic. We observed that cell attachment was greatly hindered, with no detectable focal complex formation, thereby demonstrating the potency of the molecule at the concentration utilized (Fig. S1B-E). Proper integrin engagement was further confirmed on our peptidomimetic-functionalized surfaces (Fig. S2B).

Cell proliferation based on integrin subtype. In order to ensure differential cell survival mediated by engagement of specific integrin subtypes was not due to integrin subtype specific-mediated proliferation effects, we monitored cell proliferation over the time course of the experiment and observed no differences between cells on Fn engaging integrin $\alpha_5\beta_1$, integrin $\alpha_v\beta_3$, or both, compared to initial seeding (Fig. S4).

Supplementary Figures

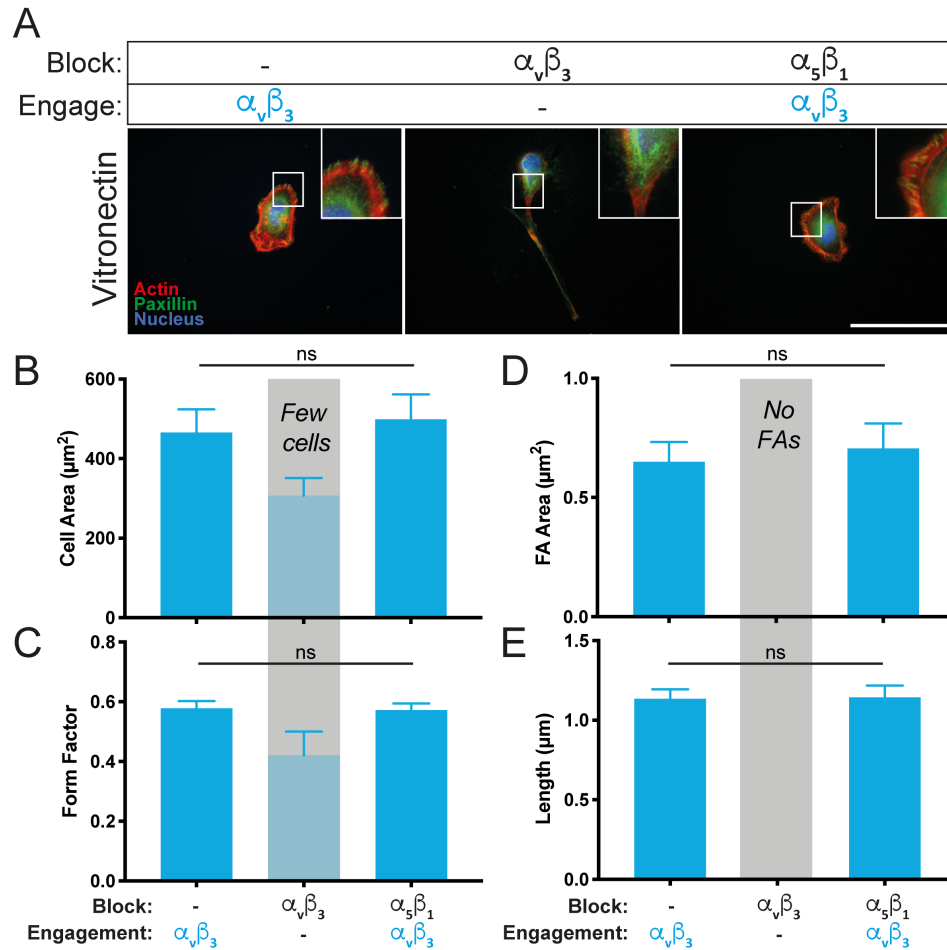


Figure S1: Cells plated on vitronectin confirm peptidomimetic functionality. (A) MDA-MB-231s were plated on immobilized vitronectin with the following conditions: no blocking peptidomimetics engages $\alpha_v\beta_3$ [left], blocking of $\alpha_v\beta_3$ results in engagement of no integrins [middle], and blocking of $\alpha_5\beta_1$ results in engagement of $\alpha_v\beta_3$ (no difference from no blocking case) [right]. Cells were stained for actin (red), paxillin (green), and nucleus (blue). Insets show zoomed in focal adhesions Scale bar: 50 μm . Cell morphology in terms of cell area (B) and form factor (C) was quantified for no blocking (i.e. $\alpha_v\beta_3$ engagement), $\alpha_v\beta_3$ blocking (i.e. no integrin engagement), and $\alpha_5\beta_1$ blocking (i.e. $\alpha_v\beta_3$ engagement). Focal adhesion (FA) morphology in terms of area (D) and major axis length (E) was quantified for all conditions as in (B, C). Blocking $\alpha_v\beta_3$ engagement resulted in very few cells attached to the surface as indicated by the gray bar; FA area could not be calculated. $n_{\text{cells (no blocking)}} = 246$; $n_{\text{cells ($\alpha_v\beta_3$ blocking)}} = 20$; $n_{\text{cells ($\alpha_5\beta_1$ blocking)}} = 312$. $n_{\text{FAs}} > 620$. Data is mean \pm 95% CI. ns = not significant by two-tailed t-test.

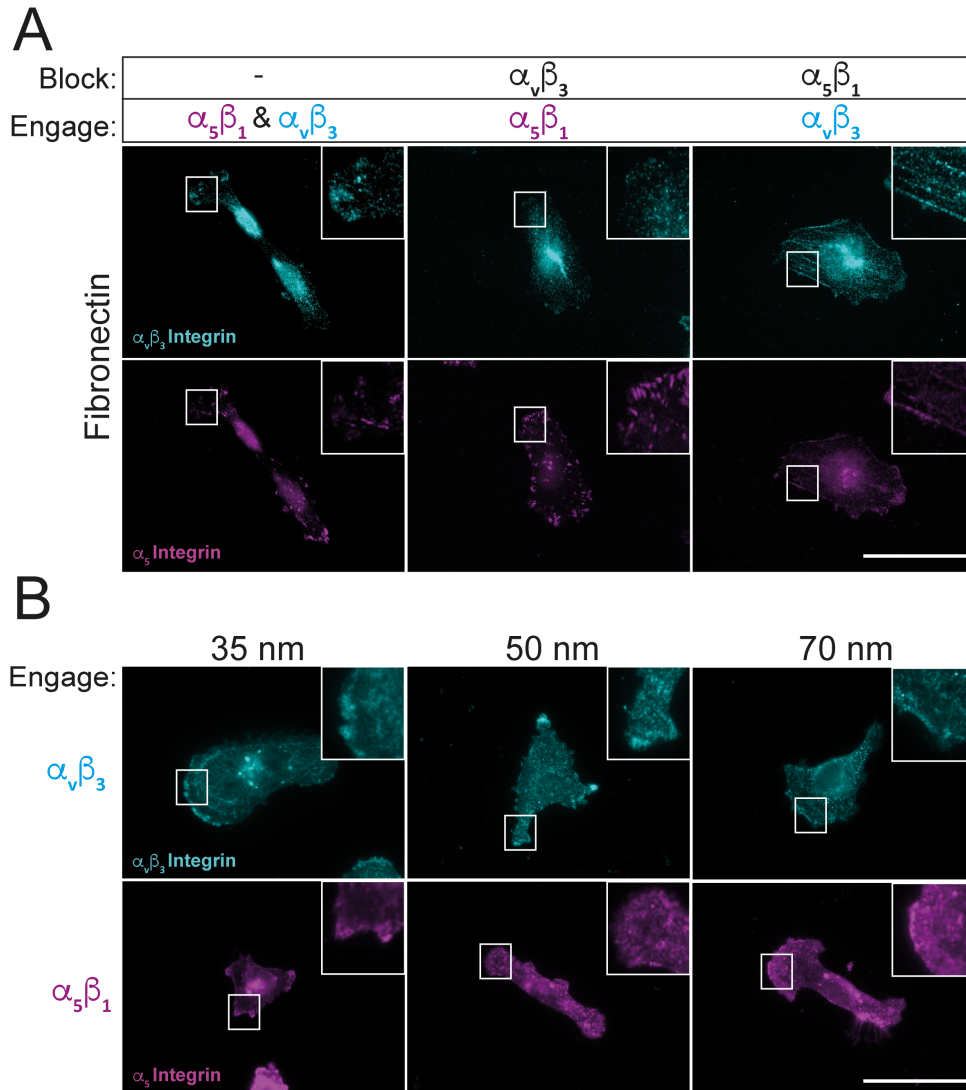


Figure S2: Integrin staining further confirms peptidomimetic functionality. (A) MDA-MB-231s were plated on immobilized fibronectin and treated with blocking peptidomimetics in order to control integrin subtype-specific engagement, i.e. no blocking engages both $\alpha_5\beta_1$ and $\alpha_v\beta_3$ (left), blocking $\alpha_v\beta_3$ engages $\alpha_5\beta_1$ (middle), or blocking $\alpha_5\beta_1$ engages $\alpha_v\beta_3$ (right). Corresponding immunofluorescence images of dual-stained cells for $\alpha_v\beta_3$ integrin (blue, top panel) and α_5 integrin (purple, bottom panel) show proper integrin engagement. Insets show zoomed in areas of the same region in each matched panel. (B) MDA-MB-231s plated on AuNPs at 35 (left), 50 (middle), or 70 (right) nm interspacing. Cells on AuNPs functionalized with $\alpha_v\beta_3$ peptidomimetic (blue, top panel) were stained for corresponding integrin expression of $\alpha_v\beta_3$ integrin (blue). Cells on AuNPs functionalized with $\alpha_5\beta_1$ peptidomimetic (purple, bottom panel) were stained for corresponding integrin expression of α_5 integrin (purple). Insets show zoomed in areas. Scale bar: 50 μ m.

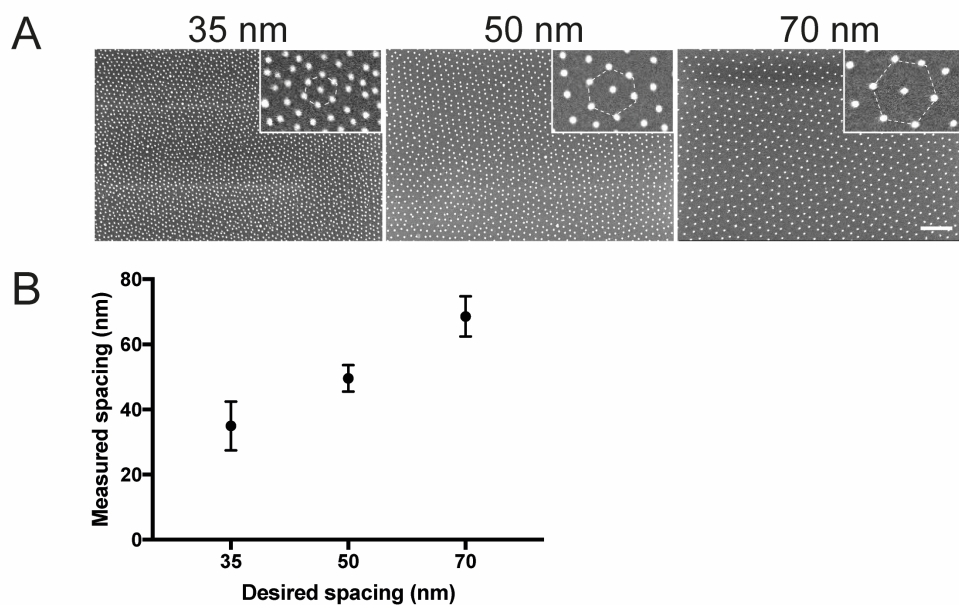


Figure S3: Block copolymer micelle nanolithography creates highly ordered, hexagonally-arranged gold nanostructures with specific interparticle spacing. (A) Representative SEM images of gold nanoparticles (AuNPs) interspaced at 35 nm (left), 50 nm (middle), and 70 nm (right). Inset shows a higher magnification with hexagonal order. Scale bar: 250 nm. (B) Characterization of interparticle spacing showing measured vs. desired spacing, i.e. 35 nm = 34.94 ± 5.31 nm; 50 nm = 49.55 ± 7.96 nm; 70 nm = 68.59 ± 12.08 nm from $n_{\text{samples}} = 5$ and $n_{\text{AuNPs}} \sim 600 - 2,500$ per sample, depending on spacing. Data is mean \pm 95% CI.

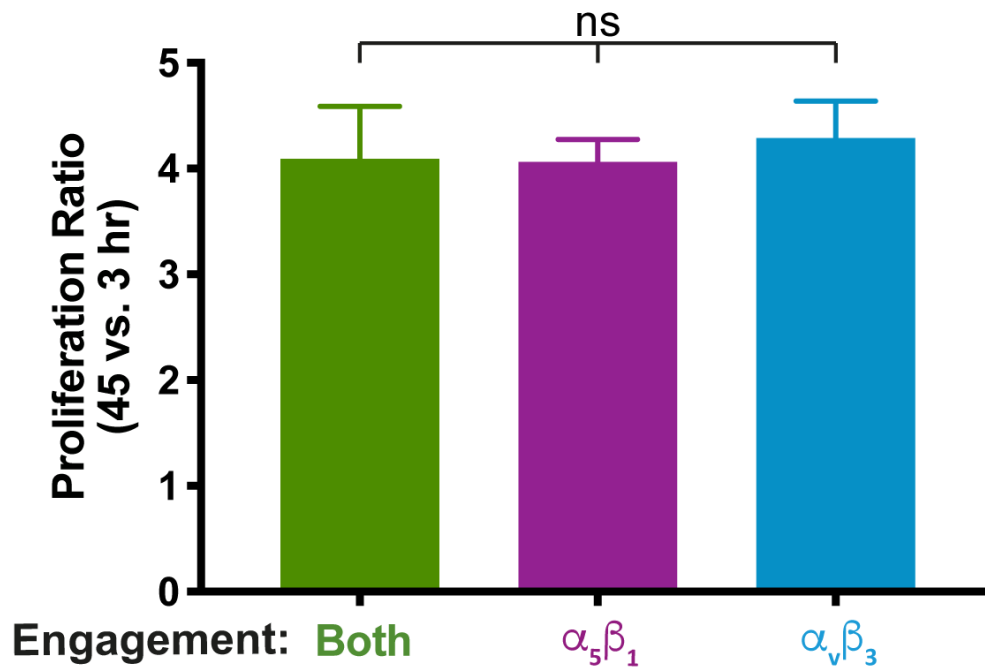


Figure S4: Cellular proliferation does not depend on integrin subtype. Proliferation ratio (45 hr normalized to 3 hr) of integrin subtype-specific engagement (Both, i.e. $\alpha_5\beta_1$ and $\alpha_V\beta_3$: green; $\alpha_5\beta_1$: purple; $\alpha_V\beta_3$: blue). Data is mean \pm 95% CI. ns = no significance by one-way ANOVA.

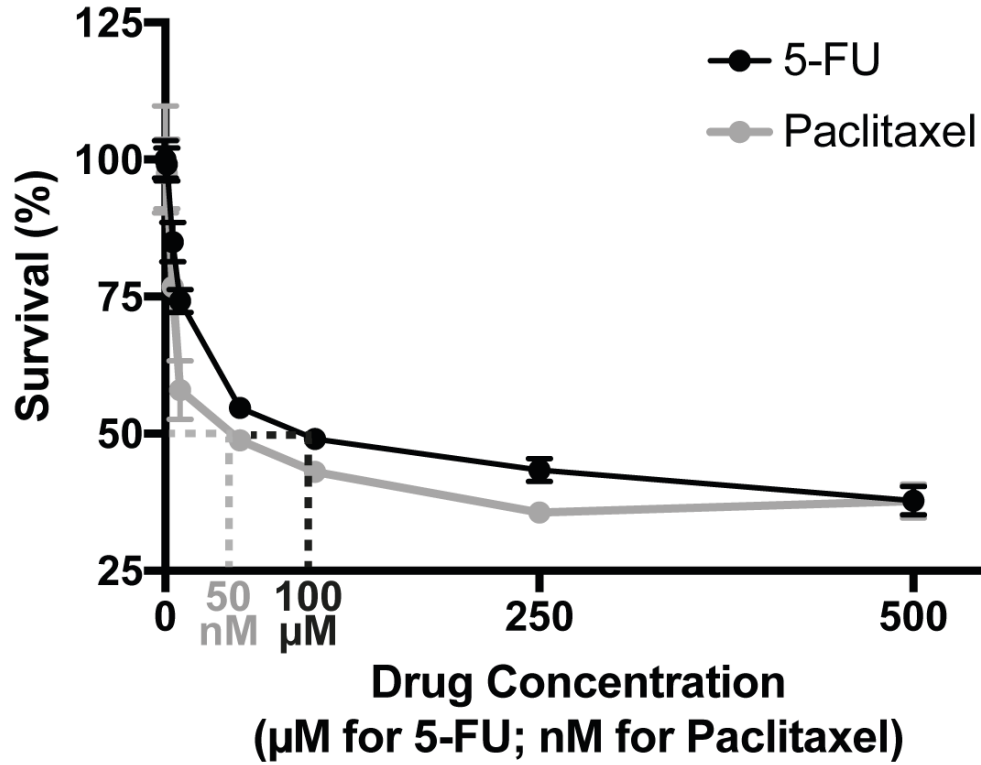


Figure S5: Drug dose curve. Percent survival of MDA-MB-231s plated on tissue culture plastic vs. concentration of drug, 5-FU (black) or Paclitaxel (gray), after 48 hr. Dashed lines indicate where approximately 50 % of the cells survive, i.e. 50 nM for Paclitaxel and 100 μM for 5-FU. Data is mean \pm sem.

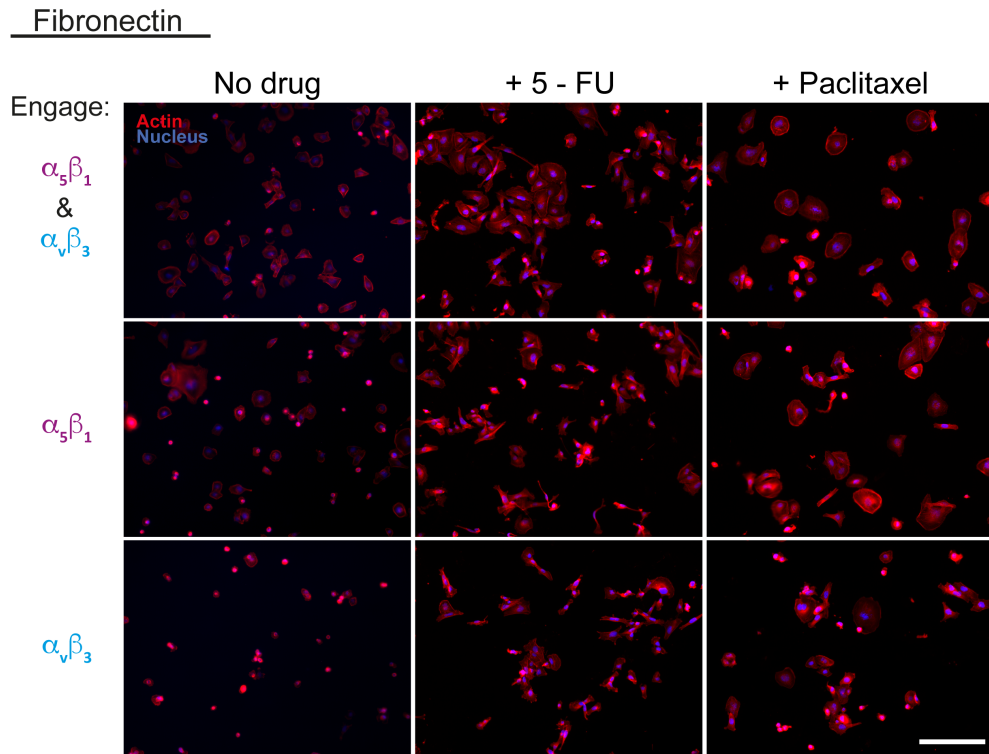


Figure S6: Low magnification images of cells plated on fibronectin. MDA-MB-231s were plated on immobilized fibronectin and treated with blocking peptidomimetics as follows: no blocking peptidomimetics engages both integrins [top row], blocking of $\alpha_v\beta_3$ results in engagement of $\alpha_5\beta_1$ (purple) [middle row], and blocking of $\alpha_5\beta_1$ results in engagement of $\alpha_v\beta_3$ (blue) [bottom row] with or without drug treatment (no drug: left column; + 5-FU: middle column; + paclitaxel: right column). Cells were stained for actin (red) and nucleus (blue). Scale bar: 200 μm .

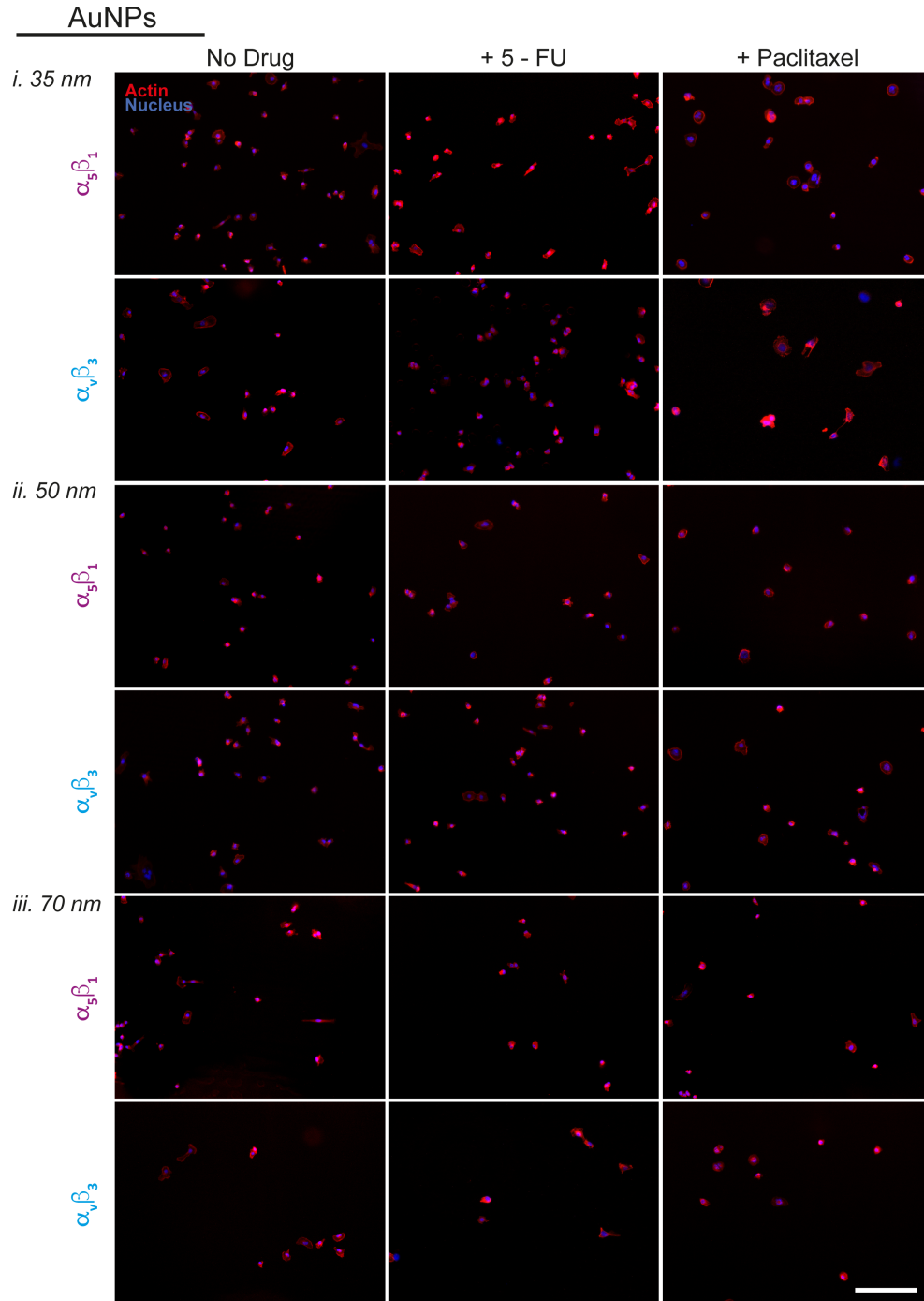


Figure S7: Low magnification images of cells plated on gold nanoparticle arrays. MDA-MB-231s were plated on AuNPs with interspacings of (i.) 35 nm, (ii.) 50 nm, or (iii.) 70 nm functionalized with integrin-specific peptidomimetics, i.e. $\alpha_5\beta_1$ (purple) or $\alpha_v\beta_3$ (blue), with or without drug treatment (no drug: left column; + 5-FU: middle column; + paclitaxel: right column). Cells were stained for actin (red) and nucleus (blue). Scale bar: 200 μm .

Tables of Significance

All significance comparisons by one-way ANOVA are displayed for experiments in Figure 1C-F (Table S1) and Figure 2C-F (Table S2).

Table S1: Table of significance of cells plated on fibronectin from all conditions (from Fig. 1C-F)

Tukey's multiple comparisons test	Cell Area		Cell Form Factor		FA Area		FA Length	
	Summary	P Value	Summary	P Value	Summary	P Value	Summary	P Value
Both vs. Both + 5-FU	ns	>0.9999	****	<0.0001	****	<0.0001	***	0.0009
Both vs. Both + Paclitaxel	***	0.0009	ns	0.6135	ns	0.2683	ns	0.071
Both vs. $\alpha 5\beta 1$	ns	0.9995	****	<0.0001	ns	0.9658	ns	>0.9999
Both vs. $\alpha v\beta 3$	****	<0.0001	****	<0.0001	****	<0.0001	****	<0.0001
Both + 5-FU vs. Both + Paclitaxel	****	<0.0001	****	<0.0001	ns	0.4952	ns	0.9894
Both + 5-FU vs. $\alpha 5\beta 1$ + 5-FU	ns	0.2096	****	<0.0001	ns	0.3011	ns	0.5976
Both + 5-FU vs. $\alpha v\beta 3$ + 5-FU	***	0.0001	*	0.0419	*	0.034	ns	>0.9999
Both + Paclitaxel vs. $\alpha 5\beta 1$ + Paclitaxel	ns	>0.9999	ns	0.5247	*	0.0184	ns	0.9966
Both + Paclitaxel vs. $\alpha v\beta 3$ + Paclitaxel	****	<0.0001	ns	0.3276	ns	0.8215	*	0.0194
$\alpha 5\beta 1$ vs. $\alpha 5\beta 1$ + 5-FU	ns	0.9924	****	<0.0001	****	<0.0001	****	<0.0001
$\alpha 5\beta 1$ vs. $\alpha 5\beta 1$ + Paclitaxel	***	0.0003	***	0.0002	****	<0.0001	**	0.0057
$\alpha 5\beta 1$ vs. $\alpha v\beta 3$	****	<0.0001	ns	0.2784	****	<0.0001	****	<0.0001
$\alpha 5\beta 1$ + 5-FU vs. $\alpha 5\beta 1$ + Paclitaxel	****	<0.0001	****	<0.0001	ns	0.9363	ns	0.3387
$\alpha 5\beta 1$ + 5-FU vs. $\alpha v\beta 3$ + 5-FU	ns	0.2705	ns	0.9857	ns	0.9789	ns	0.3876
$\alpha 5\beta 1$ + Paclitaxel vs. $\alpha v\beta 3$ + Paclitaxel	****	<0.0001	ns	>0.9999	****	<0.0001	***	0.0001
$\alpha v\beta 3$ vs. $\alpha v\beta 3$ + 5-FU	*	0.034	****	<0.0001	ns	0.9722	****	<0.0001
$\alpha v\beta 3$ vs. $\alpha v\beta 3$ + Paclitaxel	****	<0.0001	****	<0.0001	****	<0.0001	****	<0.0001
$\alpha v\beta 3$ + 5-FU vs. $\alpha v\beta 3$ + Paclitaxel	ns	0.1203	****	<0.0001	****	<0.0001	**	0.005

Table S2: Table of significance for cells plated on AuNPs from all conditions (from Fig. 2C-F)

Tukey's multiple comparisons test	Cell Area		Cell Form Factor		FA Area		FA Length	
	Summary	P Value	Summary	P Value	Summary	P Value	Summary	P Value
35 nm $\alpha 5\beta 1$ vs. 35 nm $\alpha 5\beta 1$ + 5-FU	ns	0.9786	****	<0.0001	ns	0.9997	ns	0.9839
35 nm $\alpha 5\beta 1$ vs. 35 nm $\alpha 5\beta 1$ + Paclitaxel	ns	0.7849	*	0.0221	ns	>0.9999	ns	>0.9999
35 nm $\alpha 5\beta 1$ vs. 50 nm $\alpha 5\beta 1$	**	0.005	***	0.0001	ns	0.5058	ns	>0.9999
35 nm $\alpha 5\beta 1$ vs. 70 nm $\alpha 5\beta 1$	*	0.0129	****	<0.0001	*	0.027	ns	0.8435
35 nm $\alpha 5\beta 1$ vs. 35 nm $\alpha v\beta 3$	ns	>0.9999	***	0.0004	ns	0.6411	ns	0.944
35 nm $\alpha 5\beta 1$ + 5-FU vs. 35 nm $\alpha 5\beta 1$ + Paclitaxel	ns	0.1932	****	<0.0001	ns	>0.9999	ns	0.9999
35 nm $\alpha 5\beta 1$ + 5-FU vs. 50 nm $\alpha 5\beta 1$ + 5-FU	ns	>0.9999	ns	>0.9999	ns	0.2562	*	0.016
35 nm $\alpha 5\beta 1$ + 5-FU vs. 70 nm $\alpha 5\beta 1$ + 5-FU	ns	0.7976	ns	>0.9999	ns	0.9578	ns	>0.9999
35 nm $\alpha 5\beta 1$ + 5-FU vs. 35 nm $\alpha v\beta 3$ + 5-FU	*	0.0159	****	<0.0001	ns	>0.9999	ns	>0.9999
35 nm $\alpha 5\beta 1$ + Paclitaxel vs. 50 nm $\alpha 5\beta 1$ + Paclitaxel	ns	0.9871	****	<0.0001	ns	>0.9999	ns	0.9992
35 nm $\alpha 5\beta 1$ + Paclitaxel vs. 70 nm $\alpha 5\beta 1$ + Paclitaxel	*	0.0334	ns	0.4643	ns	0.2703	ns	0.961
35 nm $\alpha 5\beta 1$ + Paclitaxel vs. 35 nm $\alpha v\beta 3$ + Paclitaxel	*	0.0118	ns	0.9422	**	0.0049	****	<0.0001
50 nm $\alpha 5\beta 1$ vs. 50 nm $\alpha 5\beta 1$ + 5-FU	ns	>0.9999	ns	>0.9999	ns	>0.9999	ns	0.6595
50 nm $\alpha 5\beta 1$ vs. 50 nm $\alpha 5\beta 1$ + Paclitaxel	ns	0.5508	**	0.0031	ns	0.9998	ns	0.8078
50 nm $\alpha 5\beta 1$ vs. 70 nm $\alpha 5\beta 1$	ns	>0.9999	ns	0.184	ns	0.9917	ns	0.4513
50 nm $\alpha 5\beta 1$ vs. 50 nm $\alpha v\beta 3$	ns	>0.9999	****	<0.0001	ns	>0.9999	ns	0.9586
50 nm $\alpha 5\beta 1$ + 5-FU vs. 50 nm $\alpha 5\beta 1$ + Paclitaxel	ns	0.9941	ns	0.409	ns	0.9973	*	0.0297
50 nm $\alpha 5\beta 1$ + 5-FU vs. 70 nm $\alpha 5\beta 1$ + 5-FU	ns	>0.9999	ns	>0.9999	ns	>0.9999	ns	0.3326
50 nm $\alpha 5\beta 1$ + 5-FU vs. 50 nm $\alpha v\beta 3$ + 5-FU	ns	0.9929	***	0.0001	ns	0.9278	ns	>0.9999
50 nm $\alpha 5\beta 1$ + Paclitaxel vs. 70 nm $\alpha 5\beta 1$ + Paclitaxel	ns	0.8007	****	<0.0001	ns	0.8505	ns	>0.9999
50 nm $\alpha 5\beta 1$ + Paclitaxel vs. 50 nm $\alpha v\beta 3$ + Paclitaxel	ns	>0.9999	****	<0.0001	ns	0.9521	ns	0.9931
70 nm $\alpha 5\beta 1$ vs. 70 nm $\alpha 5\beta 1$ + 5-FU	ns	>0.9999	ns	>0.9999	ns	0.9999	ns	>0.9999
70 nm $\alpha 5\beta 1$ vs. 70 nm $\alpha 5\beta 1$ + Paclitaxel	ns	>0.9999	**	0.0025	ns	>0.9999	ns	>0.9999
70 nm $\alpha 5\beta 1$ vs. 70 nm $\alpha v\beta 3$	***	0.0004	ns	>0.9999	*	0.0208	ns	>0.9999
70 nm $\alpha 5\beta 1$ + 5-FU vs. 70 nm $\alpha v\beta 3$ + 5-FU	****	<0.0001	*	0.019	ns	0.997	ns	>0.9999
70 nm $\alpha 5\beta 1$ + Paclitaxel vs. 70 nm $\alpha v\beta 3$ + Paclitaxel	ns	0.8176	***	0.0005	ns	0.3262	ns	0.1176
35 nm $\alpha v\beta 3$ vs. 35 nm $\alpha v\beta 3$ + 5-FU	**	0.0027	*	0.0169	ns	0.2051	ns	>0.9999
35 nm $\alpha v\beta 3$ vs. 35 nm $\alpha v\beta 3$ + Paclitaxel	****	<0.0001	**	0.0032	****	<0.0001	***	0.0001
35 nm $\alpha v\beta 3$ vs. 50 nm $\alpha v\beta 3$	ns	0.3456	****	<0.0001	ns	>0.9999	ns	0.0743
35 nm $\alpha v\beta 3$ vs. 70 nm $\alpha v\beta 3$	ns	0.9986	ns	0.7972	ns	0.5599	ns	>0.9999
35 nm $\alpha v\beta 3$ + 5-FU vs. 35 nm $\alpha v\beta 3$ + Paclitaxel	****	<0.0001	ns	>0.9999	ns	0.9214	****	<0.0001

35 nm $\alpha v\beta 3$ + 5-FU vs. 50 nm $\alpha v\beta 3$ + 5-FU	ns	>0.9999	ns	0.9973	ns	>0.9999	ns	0.7926
35 nm $\alpha v\beta 3$ + 5-FU vs. 70 nm $\alpha v\beta 3$ + 5-FU	****	<0.0001	****	<0.0001	ns	>0.9999	ns	>0.9999
35 nm $\alpha v\beta 3$ + Paclitaxel vs. 50 nm $\alpha v\beta 3$ + Paclitaxel	****	<0.0001	*	0.0271	****	<0.0001	****	<0.0001
35 nm $\alpha v\beta 3$ + Paclitaxel vs. 70 nm $\alpha v\beta 3$ + Paclitaxel	****	<0.0001	****	<0.0001	****	<0.0001	****	<0.0001
50 nm $\alpha v\beta 3$ vs. 50 nm $\alpha v\beta 3$ + 5-FU	ns	0.5617	ns	0.0583	ns	0.9686	ns	>0.9999
50 nm $\alpha v\beta 3$ vs. 50 nm $\alpha v\beta 3$ + Paclitaxel	ns	0.0641	ns	0.5716	ns	>0.9999	ns	0.9991
50 nm $\alpha v\beta 3$ vs. 70 nm $\alpha v\beta 3$	***	0.0001	****	<0.0001	ns	0.699	***	0.0003
50 nm $\alpha v\beta 3$ + 5-FU vs. 50 nm $\alpha v\beta 3$ + Paclitaxel	***	0.0002	***	0.0003	ns	0.761	ns	0.9871
50 nm $\alpha v\beta 3$ + 5-FU vs. 70 nm $\alpha v\beta 3$ + 5-FU	****	<0.0001	****	<0.0001	ns	>0.9999	ns	0.7417
50 nm $\alpha v\beta 3$ + Paclitaxel vs. 70 nm $\alpha v\beta 3$ + Paclitaxel	ns	>0.9999	****	<0.0001	ns	0.3296	ns	0.9998
70 nm $\alpha v\beta 3$ vs. 70 nm $\alpha v\beta 3$ + 5-FU	ns	0.1414	*	0.0269	ns	>0.9999	ns	0.999
70 nm $\alpha v\beta 3$ vs. 70 nm $\alpha v\beta 3$ + Paclitaxel	ns	0.9992	ns	>0.9999	****	<0.0001	**	0.006
70 nm $\alpha v\beta 3$ + 5-FU vs. 70 nm $\alpha v\beta 3$ + Paclitaxel	*	0.0257	ns	0.7521	****	<0.0001	ns	0.9242

Supporting References:

- (1) Glass, R.; Möller, M.; Spatz, J. P. Block Copolymer Micelle Nanolithography. *Nanotechnology* **2003**, 14, 1153–1160.
- (2) Williges, C.; Chen, W.; Morhard, C.; Spatz, J. P.; Brunner, R. Increasing the Order Parameter of Quasi-Hexagonal Micellar Nanostructures by Ultrasound Annealing. *Langmuir* **2013**, 29, 989–993.
- (3) Schindelin, J.; Arganda-Carreras, I.; Frise, E.; Kaynig, V.; Longair, M.; Pietzsch, T.; Preibisch, S.; Rueden, C.; Saalfeld, S.; Schmid, B.; et al. Fiji: An Open-Source Platform for Biological-Image Analysis. *Nature Methods* **2012**, 9, 676–682.
- (4) Carpenter, A. E.; Jones, T. R.; Lamprecht, M. R.; Clarke, C.; Kang, I. H.; Friman, O.; Guertin, D. A.; Chang, J. H.; Lindquist, R. A.; Moffat, J.; et al. CellProfiler: Image Analysis Software for Identifying and Quantifying Cell Phenotypes. *Genome Biology* **2006**, 7, R100.
- (5) Rechenmacher, F.; Neubauer, S.; Polleux, J.; Mas-Moruno, C.; De Simone, M.; Cavalcanti-Adam, E. A.; Spatz, J. P.; Fässler, R.; Kessler, H. Functionalizing $\alpha v\beta 3$ - or $\alpha 5\beta 1$ -Selective Integrin Antagonists for Surface Coating: A Method to Discriminate Integrin Subtypes In Vitro. *Angewandte Chemie International Edition* **2013**, 52, 1572–1575.